FT-IR Investigation of OH···N ⇌ O⁻···H⁺N Hydrogen Bonds with Large Proton Polarizability in Phosphinic Acid + N-Base Systems in the Middle and Far Infrared Region

Roland Langner and Georg Zundel*

Institute of Physical Chemistry, University of Munich, Theresienstrasse 41, D-80333 Munich, Germany

Received: February 11, 1998; In Final Form: June 1, 1998

Sixteen 1:1 dimethylphosphinic acid + N-base systems were studied in acetonitrile−chloroform (1:2) solutions as a function of the basicity of the N-bases. The complexes were measured in the middle infrared (MIR) and far-infrared (FIR) region at 20 °C and at −40 °C. The observed IR continua demonstrate that in the systems with the weaker bases an asymmetrical double minimum proton potential with the deeper well at the acid site is present. With increasing basicity the well at the base site becomes deeper and deeper and the proton potentials obtain a more symmetrical shape. The largest proton polarizability is attained with the system that shows the (on the average) most symmetrical proton potential, as indicated by the maximum bathochromic shift of the IR continuum. This shift toward lower wavenumbers is largest with the dimethylphosphinic acid + triallylamine complex. The most intense integrated absorbance of the IR continuum is also observed in this system. The characteristic intensity distribution at the symmetry point indicates medium-strong and relatively long OH···N ⇌ O⁻···H⁺N hydrogen bonds. With further increasing basicity the proton potential becomes asymmetrical again, but now with the deeper well at the base site. The proton transfer was studied considering the PO stretching vibration bands. The simultaneous observation of the acid as well as the acid anion PO bands reflect a proton-transfer equilibrium between the nonpolar and polar structure. The far-IR region demonstrates that in the most symmetrical cases the IR continua extend down to about 100 cm^{-1}. Moreover, in contrast to the results with other families of systems, it was for the first time possible to distinguish the nonpolar and polar structure in the far-IR region. Furthermore, the position of the hydrogen bond vibration indicates a significant trend of the force constant. The precise evaluation shows that the system with the (on the average) most symmetrical hydrogen bonds is achieved with a little weaker base than triallylamine, showing the largest bathochromic shift of the IR continuum.

1. Introduction

In the last 20 years a large number of acid + base families of systems in very different ΔpK_a regions have been investigated by FT-IR spectroscopy.[1−11] The ΔpK_a value is defined by the difference of the pK_a values of the protonated base and the acid (pK_a(base) − pK_a(acid)). Therefore, if one investigates a family of systems, this value is a good parameter for the representation of qualitative trends of experimental data with increasing proton transfer. This may be, for example, the intensity distribution of the IR continua, the integrated absorbance of the IR continua, or the position of the hydrogen bond vibrations. For the investigation of such families of systems the acid or the base will be kept constant, whereas the corresponding partner and hence the ΔpK_a value is varied. In this way we investigated various families of systems with strong hydrogen bonds and single minimum proton potentials, as well as with much weaker hydrogen bonds and double minimum proton potentials.

The most important result of these studies was that in the first case with increasing ΔpK_a value a single minimum is shifted continuously from the donor to the acceptor. In the second case a double minimum is changed in a way that first the deeper well occurs at the donor and then, with increasing ΔpK_a value, at the acceptor. In consequence, the proton transfer in methanesulfonic acid + *N*-oxide systems with short O··H··O hydrogen bonds can be observed as a continuous change of the vibrational bands of the acid group to the bands of the acid anion group.[8,10] The IR-spectroscopic localization of the system in which 50% proton transfer occurs, equivalent to the most symmetrical distribution of the proton in the hydrogen bond, is, however, not possible. In contrast to this spectral behavior the proton transfer in a family of systems with longer OH···N ⇌ O⁻···H⁺N hydrogen bonds is observed as a proton-transfer equilibrium. In this case the two proton limiting structures can be distinguished by different vibrational bands in the MIR spectrum.

Another point of interest is that the hydrogen bond vibration (ν_{HB}) in the far-IR region may demonstrate very different spectral features. In some families of systems this transition reflects a trend in the value of the force constant with increasing ΔpK_a,[5,7] while in other families of systems mass effects occur.[12] Furthermore, methanesulfonic acid + sulfoxide (phosphine oxide, arsine oxide) systems show a very unusual broadening effect of the ν_{HB} transition.[10] The experimentel data show that in the most symmetrical system the ν_{HB} band even merges in the intense far-IR continuous absorption. A further interesting question is whether in long hydrogen bonds with double minimum proton potentials two ν_{HB} bands can be distinguished caused by the two proton limiting structures. Up to this time no hydrogen bond vibration of the nonpolar and the polar structure could be observed in any investigated system.

In the present investigation a large number of dimethylphosphinic acid + amine systems were studied in the MIR as well as in the far-IR region. The whole family of systems comprises

* Address correspondence to this author at: Bruno-Walter-Str. 2, A-5020 Salzburg, Austria.

S1089-5639(98)01097-4 CCC: $15.00
Published on Web 07/29/1998

TABLE 1: Investigated Systems

system no. and abbreviation	full name of the base	pK_a[13]	ΔpK_a
1. DMP+CNMDEA	cyanomethyldiethylamine	4.55	1.47
2. DMP+CNEDMA	2-cyanoethyldimethylamine	7.00	3.92
3. DMP+MMor	1-methylmorpholine	7.38	4.30
4. DMP+EMor	1-ethylmorpholine	7.67	4.59
5. DMP+TAlA	triallylamine	8.31	5.23
6. DMP+DMBzA	dimethylbenzylamine	8.91	5.83
7. DMP+DEBzA	diethylbenzylamine	9.44	6.36
8. DMP+TBA	tri-*n*-butylamine	9.93	6.85
9. DMP+MPip	1-methylpiperidine	10.08	7.00
10. DMP+DEMA	diethylmethylamine	10.46	7.38
11. DMP+TEA	triethylamine	10.75	7.67
12. DMP+PMPip	1,2,2,6,6-pentamethylpiperidine	11.25[14]	8.17
13. DMP+DBU	1,8-diazabicyclo[5.4.0]undec-7-ene	11.90[15]	8.82
14. DMP+MTBD	1,3,4,6,7,8-hexahydro-1-methyl-2*H*-pyrimido[1,2-*a*]pyrimidine	13.00[15]	9.92

a ΔpK_a range of over 8 units. Relatively long hydrogen bonds with double minimum proton potentials could be expected, since the dimethylphosphinic acid belongs to the group of weak organic acids. The high number of systems was necessary for the exact localization of the most symmetrical system, i.e., the maximum bathochromic shift of the IR continuum. Moreover, the evaluation and interpretation of the far-IR region was supported by the comparison of the far-IR results with respective results obtained with other families.

2. Results and Discussion

2.1. Infrared Continuum and Proton Potential. In Table 1, all investigated systems with the corresponding abbreviations and the ΔpK_a values are given. Dimethylphosphinic acid (DMP) has a pK_a value of 3.08.[16] In all cases 0.5 mol dm^{-3} 1:1 acid + base mixtures in acetonitrile−chloroform (1:2) solution were studied. The spectra were taken from the solutions at 20 °C and at −40 °C. In Figure 1, eight selected systems are shown in the whole IR region from 4000 to 100 cm^{-1}. In this way the changes of the IR continua with increasing ΔpK_a value can be followed very well. It is important to determine the system with the largest symmetry of the proton potential, i.e., the system with the largest proton polarizability. This system shows the largest bathochromic shift of the continuum and provides information on the shape of the proton potential.[17,18]

First of all it should be noted that only heteroconjugated 1:1 complexes are formed. Homoconjugated complexes are not observed, since even in the most polar systems no IR continuum, caused by homoconjugated bonds, is found.[12] Only the broad ν(NH) band of the protonated N-base is found at about 2800 cm^{-1} (Figure 1h). Further evaluation demonstrates that in the system with the weakest base (**1**) at 20 °C a broad IR continuum between 3000 and 1000 cm^{-1} is present (Figure 1a). The band-like structure of the continuous absorption in the region 3000−1500 cm^{-1} is generated by Fermi resonance.[19] The three broad bands (2830 cm^{-1}, 2390 cm^{-1}, 1680 cm^{-1}) are comparable with that in the acetic acid + pyridine complex[20] and correspond to Hadzi's ABC bands caused by asymmetrical hydrogen bonds with large anharmonicity.[21−23] Considering first the continuous absorptions at 20 °C, up to system **5** the intensity of the transitions at higher wavenumbers decreases, while those at lower wavenumbers increases (Figure 1b,c). Corresponding to this spectral behavior the IR continua show a bathochromic shift. This shift of the continuous absorption toward lower wavenumbers becomes maximal in the DMP + TAlA system (**5**), i.e., at a ΔpK_a value of 5.23 (Figure 1c). In the following systems, the continuous absorption indicates again a hypsochromic shift (Figure 1d−h). The temperature-dependent measurements demonstrate that the investigated complexes react very sensitively to temperature. This is to be recognized very impressively in system **1**, in which at lower wavenumbers the IR continuum increases strongly with decreasing temperature (Figure 1a). Furthermore, with the maximum bathochromic shift of the IR continua (**5**) the temperature dependence indicates a clear hypsochromic shift (Figure 1c). In the following systems, an analogous temperature effect is observed, since with decreasing temperature the proton transfer is supported (Figure 1d−h).[24] Due to this fact a very broad ν(NH) stretching vibration band of the protonated N-base arises at about 2000 cm^{-1} (Figure 1d). This is most clearly seen in the spectra of the samples at −40 °C. With increasing ΔpK_a value, the ν(NH) band is shifted toward higher wavenumbers and becomes significantly narrower (Figure 1d−h). In summary we can state that the most interesting system is the DMP + TAlA complex (**5**) in which the highest symmetry of the proton potential and the largest proton polarizability are reached.

Considering the intensity distribution of the IR continuum in system **5** as a function of the wavenumber**,** some conclusions can be drawn on the bond length (Figure 1c):[17,18] Almost the same intensity of the continuous absorption in the region from 3000 to 500 cm^{-1} indicates medium-strong OH···N ⇌ O$^-$···H$^+$N hydrogen bonds with pronounced double minimum proton potentials. Decisive in this connection is the fact that even at the maximum bathochromic shift of the IR continuum an intense absorption remains at higher wavenumbers. This result explains also the strong temperature effect, since a double minimum proton potential reacts much more sensitively to all factors that influence the potential symmetry. For this reason the trend of the proton potential symmetry at 20 °C can be described as follows:

First, an asymmetrical double minimum with the deeper well at the acid site is present (**1**). Then, with increasing ΔpK_a value, the well at the base site becomes deeper and deeper. After passing the most symmetrical system (**5**) in which the two wells have approximately the same average depth, the proton potential becomes asymmetrical again. The deeper well is now located at the base site. Decreasing temperature causes a considerable shift in the direction of the polar structure. Corresponding to this trend of the proton potential symmetry the hydrogen bonds first contract with increasing ΔpK_a value, then obtain the smallest bond length in system **5**, and finally expand again.

After the qualitative evaluation of the spectra, in Figure 2 the integrated complex absorbance minus the corresponding base absorbance is presented. This value reflects the integrated absorbance of the continuum, since it contains additionally only the bands of the DMP which are, however, in all systems almost the same. The results show that the intergrated absorbance of the continuum first increases with increasing ΔpK_a value, then reaches a maximum in the DMP + TAlA system (**5**), and finally decreases again. Only in system **9** was a slightly too high value obtained, which is possibly due to an error in the baseline correction or an incorrect pK_a value. Thus, the complex with the largest integrated absorbance of the continuum agrees very well with the maximum bathochromic shift of the IR continuum. Furthermore, these results confirm the interpretation that in system **5** the largest proton polarizability, i.e., the highest symmetry of the proton potential, is present.

2.2. Proton Transfer and ΔG_{PT}^0 Potential. The results in section 2.1 have demonstrated that in the present series of systems medium-strong OH···N ⇌ O$^-$···H$^+$N hydrogen bonds with pronounced double minimum proton potentials occur. For

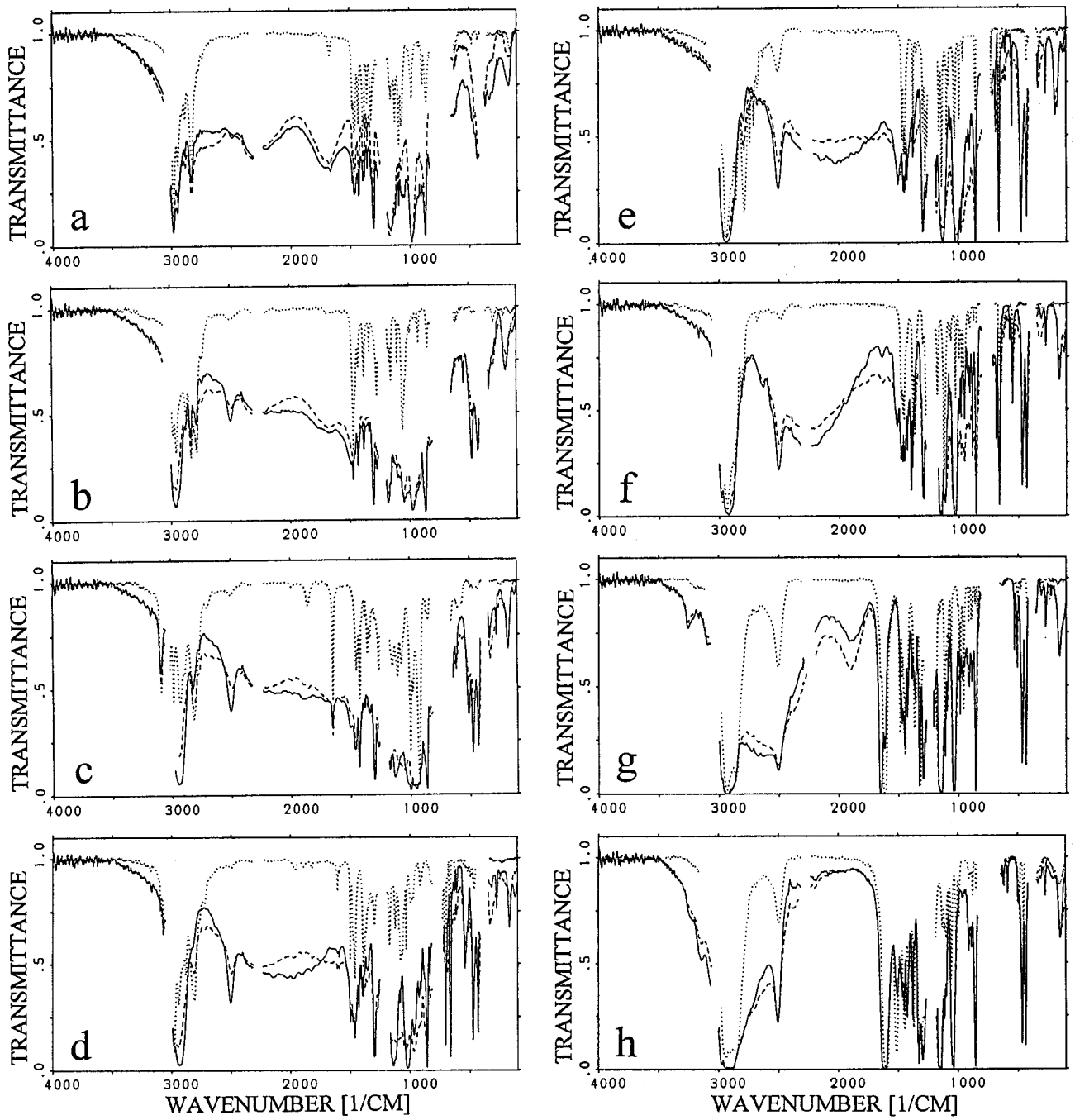

Figure 1. FT-IR spectra of the amines in acetonitrile−chloroform (1:2) at 20 °C (···) and the 1:1 DMP + amine mixtures in acetonitrile−chloroform (1:2) at 20 °C (- − -) and at −40 °C (—) in the region 4000−100 cm^{-1}; concentration 0.5 mol dm^{-3}; layer thickness 130 μm: (a) DMP + CNMDEA (**1**); (b) DMP + CNEDMA (**2**); (c) DMP + TAlA (**5**); (d) DMP + DEBzA (**7**); (e) DMP + MPip (**9**); (f) DMP + PMPip (**12**); (g) DMP + DBU (**13**); (h) DMP + MTBD (**14**).

this reason also a proton-transfer equilibrium between the two proton limiting structures should be expected. While, however, the behavior of the proton in the hydrogen bond is determined by the proton potential, the proton-transfer process is determined by the free enthalpy, i.e., the ΔG_{PT}^0 potential. So the proton transfer is followed best by the stretching vibrational bands of the acid or acid anion groups, respectively. In Figure 3 eight selected systems are shown in the IR region from 1400 to 800 cm^{-1}.

In the system with the weakest base (**1**) the ν(P═O) vibration at about 1170 cm^{-1} and the ν(P−OH) vibration at about 990 cm^{-1} are observed (Figure 3a). In this case the nonpolar structure is preferentially present at 20 °C, and the proton is located mainly in a much deeper well of the ΔG_{PT}^0 potential at the acid site ($\Delta G_{PT}^0 > 0$). Considering first the spectra at higher temperature, in the following systems the $\nu_{as}(PO_2^-)$ vibration in the region 1160−1100 cm^{-1} and the $\nu_s(PO_2^-)$ vibration in the region 1060−1000 cm^{-1} become more and more intense (Figure 3b,c). The evaluation of these bands is certainly complicated, since increasing IR continua as well as various base absorptions superimpose this spectral region. However, the experimental data show that at the earliest in the DMP + DEBzA system (**7**) a well-balanced intensity distribution between the ν(P−OH) vibration at about 960 cm^{-1} and the $\nu_s(PO_2^-)$ vibration at about 1030 cm^{-1} is observed (Figure 3d). In this system the two proton limiting structures gain obviously about the same weight, corresponding to the (on the average) most symmetrical ΔG_{PT}^0 potential ($\Delta G_{PT}^0 = 0$) or 50% proton

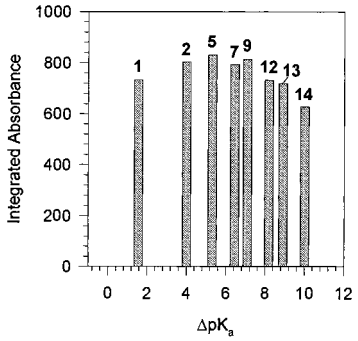

Figure 2. Change of the integrated complex absorbance minus the respective base absorbance at 20 °C with increasing ΔpK_a value; the corresponding system number is given above the bars.

transfer. Moreover, in the region between 1180 and 1080 cm^{-1} a well-balanced intensity distribution occurs. However, because of the small spectral separation of the ν(P═O) and the $\nu_{as}(PO_2^-)$ vibration, these transitions cannot be distinguished. In system **9** already the polar structure becomes dominant (Figure 3e). This is indicated by the higher intensity of the slightly bathochromically shifted $\nu_s(PO_2^-)$ vibration at about 1010 cm^{-1}, as well as by the fact that the $\nu_{as}(PO_2^-)$ vibration now arises at about 1130 cm^{-1}. With further increasing the ΔpK_a value the polar structure becomes more and more dominant. Finally, in system **14** two relatively sharp bands at about 1150 and 1030 cm^{-1} remain (Figure 3h). The proton is now located in the much deeper well of the ΔG_{PT}^0 potential at the base site ($\Delta G_{PT}^0 < 0$).

The pronounced temperature effect is already visible in system **1** (Figure 3a), since the continuous absorption increases considerably in this region. Therefore, the temperature-dependent measurements may be useful for the localization of the bands corresponding to the polar structure in the regions 1160−1100 and 1060−1000 cm^{-1} (Figure 3a−c). The evaluation of system **5**, being the system with the maximum bathochromic shift of the IR continuum, demonstrates that at 20 °C the polar structure does not yet obtain the same weight as the nonpolar structure (Figure 3c). This result is supported by the spectrum of the complex at −40 °C in which the bands of the polar structure clearly arise at about 1130 and 1020 cm^{-1}. Furthermore, in system **7** the shift of the proton transfer equilibrium in favor of the polar structure can be impressively observed (Figure 3d). The spectrum of the complex at −40 °C shows the strong increase of the $\nu_s(PO_2^-)$ vibration at about 1020 cm^{-1}, as well as the $\nu_{as}(PO_2^-)$ vibration arising at about 1140 cm^{-1}. Thus, the results in this spectral region also confirm a very strong temperature effect and indicate pronounced double minimum ΔG_{PT}^0 potentials.

Additionally, the stretching vibrational bands indicate that 50% proton transfer is only observed in the DMP + DEBzA system (**7**), i.e., at a ΔpK_a value of about 6.40. A quantitative evaluation was not possible because of the intense IR continua and various base absorptions that mask the relevant bands. So missing the exact absorption coefficients corresponding to the transitions of the nonpolar and polar structures, the system with the (on the average) most symmetrical ΔG_{PT}^0 potential could only be estimated. This was done assuming that both coefficients have nearly the same value. In summary we can state that the maximum bathochromic shift of the IR continuum (largest proton polarizability) occurs before 50% proton transfer is reached. However, this result is still to be confirmed by ^1H NMR spectroscopic measurements.

2.3. The Hydrogen Bond Vibration in the Far-IR Region. As known from other far-IR investigations, the hydrogen bond vibration (ν_{HB}) can provide further important information on coupling mechanisms with other transitions,[10] and especially information on the trend of the force constant.[5,7] For the evaluation of this vibration in the investigated family of systems no semiempirical calculations were necessary, since the used N-bases show beside the ν_{HB} vibration, if any, only a few absorptions in the far-IR region below 300 cm^{-1}. Thus, usually only the ν_{HB} vibration is observed as an intense band. Only in the two systems DMP + MMor (**3**) and DMP + MPip (**9**) does a band splitting occur which is possibly caused by an interaction with a base vibration. In all other cases the ν_{HB} band could be clearly assigned. In Figure 4 all 14 systems are shown in the far-IR region from 600 to 100 cm^{-1}. The hydrogen bond vibrations are marked by an arrow.

First of all it should be noted that ν_{HB} appears in general as a relatively sharp band and shows no such extreme broadenig effect as it does in the MSA + sulfoxide (phosphine oxide, arsine oxide) family of systems.[10] Furthermore, the continuous absorption in the far-IR region is not as intense as in the above-mentioned series of systems. Even in the complex with the largest proton polarizability at 20 °C (**5**) only a weak continuous absorption extends down to about 100 cm^{-1} (Figure 4e). Additionally, already beginning with system **3** the IR continuum in this region decreases again at −40 °C (Figure 4c).

The exact evaluation of ν_{HB} in Figure 4 demonstrates that in most cases this band is structured at 20 °C. This is particularly true in those complexes in which the two proton limiting structures coexist with a comparable weight (Figure 4d−h). In these cases strong temperature effects occur, favoring a transition with a relatively sharp band profile. Because of this strong temperature dependence, Fermi resonance effects can be excluded. The spectral behavior rather indicates a thermodynamic equilibrium such as the proton-transfer equilibrium. This becomes possible when the proton fluctuation frequency ν^{fluc}, which depends mainly on the bond length, is shifted into the region of the resolving power of the far-IR spectroscopy (300 $cm^{-1} \approx 10^{-12}$ Hz). In this case two vibrational bands, one of a nonpolar (ν_{HB}nonpolar) and one of a polar (ν_{HB}polar) structure, should be observed. The possibility of distinguishing the two transitions is, of course, also dependent on their half-width $\Delta\nu_{HB}$ as well as their spectral separation $\delta\nu_{HB}$. Thus, only when the condition $\Delta\nu_{HB} < \delta\nu_{HB}$ is fulfilled and the coalescence point is passed can ν_{HB}nonpolar and ν_{HB}polar be resolved in the far-IR spectrum. Here, $\delta\nu_{HB}$ is influenced by various factors referring to the two proton limiting structures as, for example, force constants, specific mass effects, or the interaction with the solvent. Usually, however, only one band due to the ν_{HB} vibration was found.[1,5,10,12]

With all these considerations taken into account, in the DMP + DEBzA system (**7**) at 20 °C the two ν_{HB} transitions should be distinguished best, since in the MIR region a well-balanced proton transfer equilibrium was found. In the respective spectrum a broader band at slightly higher wavenumbers and a relatively sharp band at slightly lower wavenumbers are observed (Figure 4g). The broad band corresponds to the nonpolar structure (ν_{HB}nonpolar), while the relatively sharp band corresponds to the polar structure (ν_{HB}polar). The spectrum of the sample at −40 °C confirms this assignment, too, since with decreasing temperature ν_{HB}nonpolar vanishes almost completely, while ν_{HB}polar gains considerable intensity. This strong temperature effect agrees very well with the respective effect observed in the MIR region with the PO stretching vibration bands of the acid and acid anion. The other relevant complexes show quite similar spectral behavior in the ν_{HB} region, especially

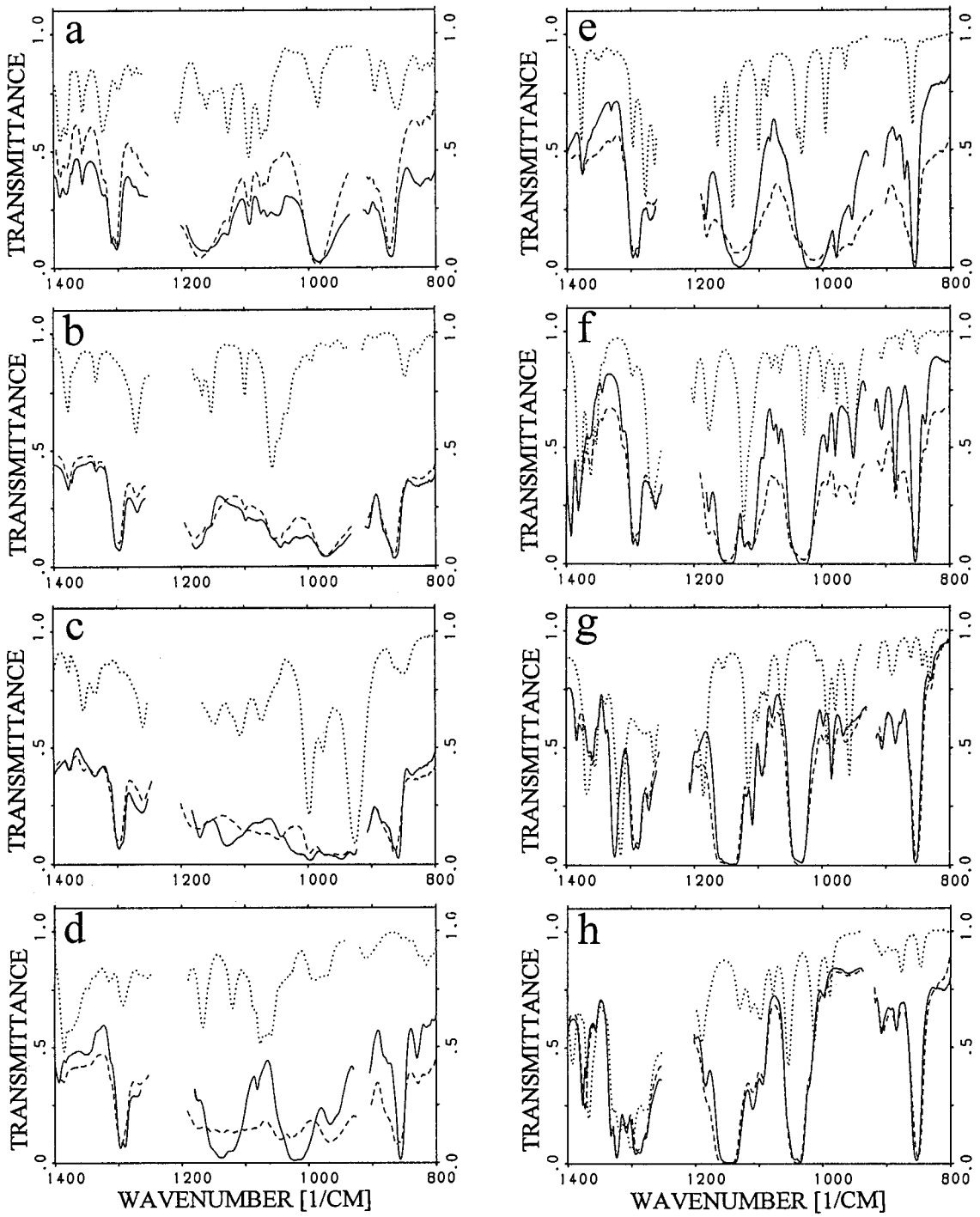

Figure 3. FT-IR spectra of the amines in acetonitrile−chloroform (1:2) at 20 °C (···) and the 1:1 DMP + amine mixtures in acetonitrile−chloroform (1:2) at 20 °C (- − -) and at −40 °C (—) in the region 1400−800 cm^{-1}; concentration 0.5 mol dm^{-3}; layer thickness 130 μm: (a) DMP + CNMDEA (**1**); (b) DMP + CNEDMA (**2**); (c) DMP + TAlA (**5**); (d) DMP + DEBzA (**7**); (e) DMP + MPip (**9**); (f) DMP + PMPip (**12**); (g) DMP + DBU (**13**); (h) DMP + MTBD (**14**).

the DMP + TAlA system (**5**) (Figure 4e). The result that the magnitude of $\delta\nu_{HB}$ is in most cases small may also explain the fact that such equilibria are generally very difficult to observe.

Because of the small $\delta\nu_{HB}$ usually only the average band positions were determined. Merely in systems **5** and **7**, which show a slightly larger difference between the two transitions at 20 °C, a bandfit was carried out. In Table 2, the band positions of ν_{HB} as well as their band shapes are given. In Figure 5, the band positions at −40 °C are shown dependent on the ΔpK_a value. It is expected, if mass effects can be neglected, that the trend of the ν_{HB} position reflects the trend of the force constant. For this reason the greatest value of the ν_{HB} position is expected in the ΔpK_a region of the system with the maximum bathochromic shift of the IR continuum. It is clearly recognizable that with increasing proton-transfer first a hypsochromic shift and, after passing a maximum, a bathochromic shift are observed. This spectral behavior of ν_{HB} is marked by dashed lines and indicates a trend of the force constant. Therefore, the strongest hydrogen bonds, equivalent to the largest force constant, are formed in the DMP + EMor complex (**4**). This result is interesting, since it shows that the strongest hydrogen bonds are probably reached slightly before the maximum bathochromic shift of the IR continuum. Thus, the trend of the bond strength reflects not exactly that of the IR continuum

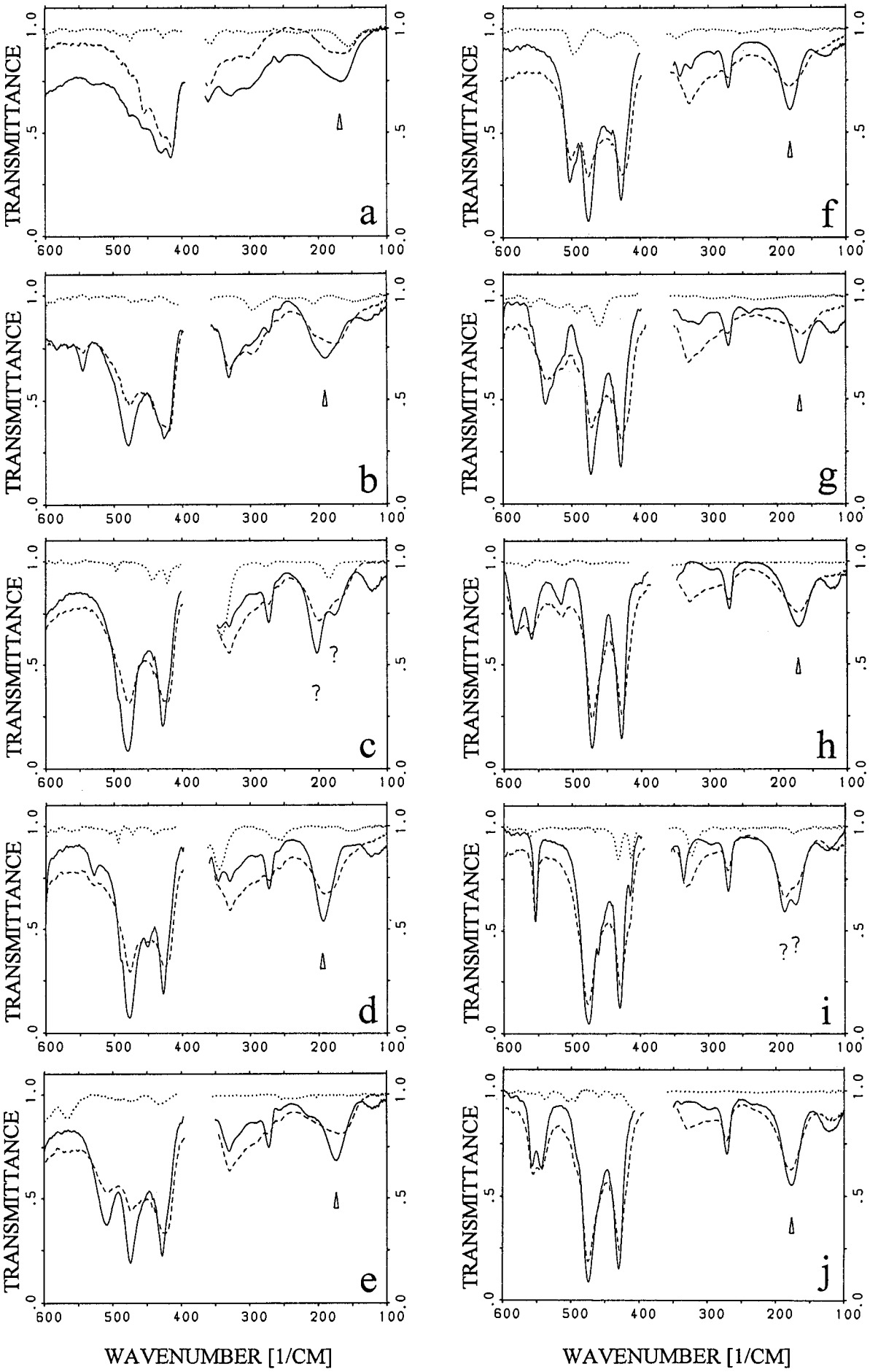
TRANSMITTANCE
1.0
.5
.0
600
500
400
300
200
100
a
b
c
?
?
d
e
f
g
h
i
??
j
WAVENUMBER [1/CM]
WAVENUMBER [1/CM]

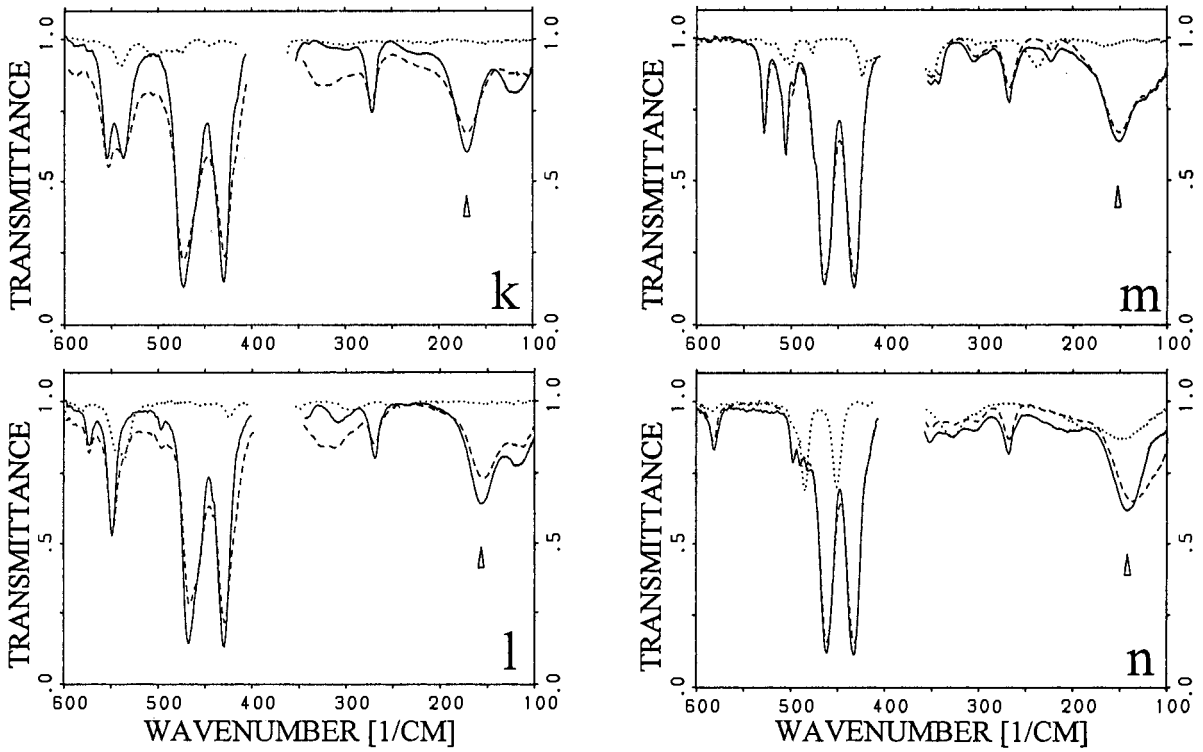

Figure 4. FT-IR spectra of the amines in acetonitrile−chloroform (1:2) at 20 °C (···) and the 1:1 DMP + amine mixtures in acetonitrile−chloroform (1:2) at 20 °C (- − -) and at −40 °C (—) in the region 600−100 cm^{-1}; concentration 0.5 mol dm^{-3}; layer thickness 130 μm: (a) DMP + CNMDEA (**1**); (b) DMP + CNEDMA (**2**); (c) DMP + MMor (**3**); (d) DMP + EMor (**4**); (e) DMP + TAlA (**5**); (f) DMP + DMBzA (**6**); (g) DMP + DEBzA (**7**); (h) DMP + TBA (**8**); (i) DMP + MPip (**9**); (j) DMP + DEMA (**10**); (k) DMP + TEA (**11**); (l) DMP + PMPip (**12**); (m) DMP + DBU (**13**); (n) DMP + MTBD (**14**).

or the proton polarizability, respectively. The deviation of some systems from the auxiliary line is caused by mass effects.

3. Experimental Section

The substances were purchased from Fluka and Aldrich. In each case, substances with the highest available purity were used. The dimethylphosphinic acid was dissolved in benzene and dried over P_4O_{10}. Then the acid was recrystallized from dry benzene. Moreover, a 3% excess of its anhydride was added to avoid water traces arising from the complex preparation. The amines were dried over molecular sieves (3 Å).

Dimethylphosphinic acid was synthesized by the reaction of phosphorus thiochloride with a Grignard methyl during ice/NaCl cooling followed by the oxidation and hydrolysis of the obtained bis(dimethylthiophosphine) with hydrogen peroxide.[25] Diethylphosphinic anhydride was synthesized by heating dimethylphosphinyl chloride with dimethylphosphinic acid ethyl ester under release of ethyl chloride.[26] While the first component was obtained by chlorination of the acid with phosphorus pentachloride, the second component was obtained by a conversion of acid chloride with sodium ethoxide. Diethylbenzylamine was synthesized by nucleophilic aliphatic substitution of benzyl chloride with diethylamine in boiling acetonitrile.[27]

All preparations and transfers of the solutions were performed in a water-free glovebox. For the IR investigations, cells with silicon windows were used, since silicon is characterized by a high chemical resistance to acids and transparent in the far-IR region. However, because of the high reflectivity of this material, wedge-shaped layers had to be applied to avoid interference patterns superimposed on the spectra. The mean layer thickness was 130 μm. The spectra of the samples were taken with a FT-IR spectrometer (Bruker IFS 113v). In the MIR region a DTGS detector (resolution 4 cm^{-1}) and in the far-IR region a He-cooled bolometer (resolution 1 cm^{-1}) were used. The solvent bands were subtracted. In the region of the strongest solvent bands the energy loss was too high to obtain any information. For the temperature-dependent measurements an ultracryomat (Lauda K 120 W) was used.

TABLE 2: Spectroscopic Data of the Hydrogen Bond Vibration (ν_{HB})[a]

	$(H_3C)_2POOH\cdots NR_3$			
	ν_{HB} [cm^{-1}]		band shape	
systems	20 °C	−40 °C	20 °C	−40 °C
DMP	184 (20 °C)		nsp (20 °C)	
1. DMP + CNMDEA	154	160	sp	sp
2. DMP + CNEDMA	181	189	sp	sp
3. DMP + MMor	(198/165)	(203/174)	anp	anp
4. DMP + EMor	187	193	sp	nsp
5. DMP + TAlA	187 + 161	174	sp	nsp
6. DMP + DMBzA	180	181	sp	nsp
7. DMP + DEBzA	195 + 161	166	sp	nsp
8. DMP+TBA	173	171	sp	nsp
9. DMP + MPip	(189/169)	(189/179)	anp	anp
10. DMP + DEMA	178	177	nsp	nsp
11. DMP + TEA	169	170	nsp	nsp
12. DMP + PMPip	154	156	nsp	nsp
13. DMP + DBU	153	153	nsp	nsp
14. DMP + MTBD	137	141	nsp	nsp
	$(H_3C)_2POO^-\cdots H^+NR_3$			

[a] sp = split; nsp = not split; anp = assignment not possible.

4. Conclusion

In the series of the DMP + amine systems the continuous absorption demonstrates that with increasing ΔpK_a value first the maximum intensity shifts toward lower wavenumbers, then reaches a maximum bathochromic shift, and after passing this point shifts toward higher wavenumbers again. This well-

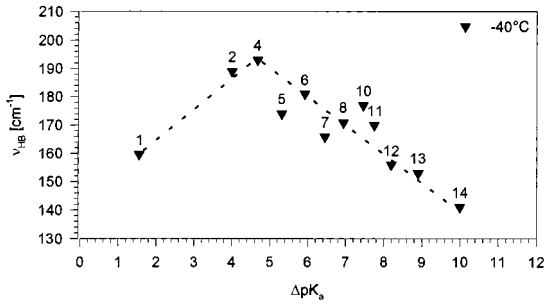

Figure 5. Trend of the hydrogen bond vibration (ν_{HB}) at −40 °C with increasing ΔpK_a value; the corresponding system number is given above the symbols.

known spectral behavior of other families of systems is also supported by the temperature-dependent measurements. With decreasing temperature, the IR continuum generally shifts in the direction of an increasing proton transfer. But in contrast to the MSA + O-base family of systems forming strong O··H··O hydrogen bonds,[10] the present series shows a clear temperature effect at the maximum bathochromic shift of the IR continuum. This spectral feature indicates a much more temperature-sensitive proton potential. Furthermore, the maximum intensity occurs in the region 3000−700 cm^{-1}. This characteristic intensity distribution of the continuous absorption indicates medium-strong OH···N ⇌ O$^-$···H$^+$N hydrogen bonds with longer ON-distances and pronounced double minimum proton potentials. At this point also the largest integrated absorbance of the IR continuum is found, and thus the largest proton polarizability. The system with the maximum bathochromic shift of the IR continuum, i.e., the system with the (on the average) most symmetrical proton potential, was identified as the DMP + TAlA complex with a ΔpK_a value of 5.23.

The PO stretching vibration bands of the acid group as well as of the acid anion group demonstrate that with increasing ΔpK_a value a proton-transfer equilibrium between the −POOH group and the $-PO_2^-$ anion group is observed. Due to the two proton limiting structures the ν(P−OH) band decreases, while the $\nu_s(PO_2^-)$ band increases. This was also supported by the enormous temperature effect showing a large increase of the polar structure with decreasing temperature. All these results indicate pronounced double minimum ΔG_{PT}^0 potentials. The system in which the nonpolar structure has approximately the same weight than the polar structure is the DMP + DEBzA complex with a ΔpK_a value of 6.36. As to whether in this system actually 50% proton transfer occurs is to be confirmed by ^{1}H NMR spectroscopy.

Most of the hydrogen bond vibrations (ν_{HB}) in the far-IR region could be assigned. The results show that in the DMP + DEBzA system two ν_{HB} transitions are observed. While the band at slightly higher wavenumbers shows a large half-width and vanishes with decreasing temperature, the other band with a much smaller half-width increases strongly at the same time. This spectral behavior indicates a proton transfer equilibrium in the far-IR region. Moreover, similar to the MSA + *N*-oxide family of systems, the position of the hydrogen bond vibration reflects a trend of the force constant. Thus, the system with the strongest hydrogen bonds is the DMP + EMor complex with a ΔpK_a value of 4.59. This result demonstrates that the greatest bond strength is probably reached already one system before the maximum bathochromic shift of the IR continuum, i.e., the system with the largest proton polarizability.

Acknowledgment. Our thanks are due to the Deutsche Forschungsgemeinschaft and the Fonds der Deutschen Chemischen Industrie for their support of this work.

References and Notes

(1) Rabold, A.; Brzezinski, B.; Langner, R.; Zundel, G. *Acta Chim. Slov.* **1997**, *44*, 237.
(2) Albrecht, G.; Zundel, G. *J. Chem. Soc., Faraday Trans. 1* **1984**, *80*, 553.
(3) Lindemann, R.; Zundel, G. *J. Chem. Soc., Faraday Trans. 2* **1977**, *73*, 788.
(4) Brzezinski, B.; Brycki, B.; Zundel, G.; Keil, T. *J. Phys. Chem.* **1991**, *95*, 8598.
(5) Keil, T.; Brzezinski, B.; Zundel, G. *J. Phys. Chem.* **1992**, *96*, 4421.
(6) Brycki, B.; Brzezinski, B.; Zundel, G.; Keil, T. *Magn. Reson. Chem.* **1992**, *30*, 507.
(7) Rabold, A.; Zundel, G. *J. Phys. Chem.* **1995**, *99*, 12158.
(8) Böhner, U.; Zundel, G. *J. Phys. Chem.* **1985**, *89*, 1408.
(9) Böhner, U.; Zundel, G. *J. Phys. Chem.* **1986**, *90*, 964.
(10) Langner, R.; Zundel, G. *J. Phys. Chem.* **1995**, *99*, 12214.
(11) Geppert, S.; Rabold, A.; Zundel, G.; Eckert, M. *J. Phys. Chem.* **1995**, *99*, 12220.
(12) Rabold, A.; Bauer, R.; Zundel, G. *J. Phys. Chem.* **1995**, *99*, 1889.
(13) Rappoport, Z. *CRC—Handbook of Tables for Organic Compound Identification*; CRC Press Inc.: Boca Raton, FL, 1985; p 436.
(14) Hall, H. K. *J. Am. Chem. Soc.* **1957**, *79*, 5444.
(15) Kubota, Y.; Hanaoka, T.; Takeuchi, K.; Sugi, Y. *Synlett* **1994**, 515.
(16) Crofts, P. C.; Kosolapoff, G. M. *J. Am. Chem. Soc.* **1953**, *75*, 3379.
(17) Zundel, G. *The Hydrogen Bond—Recent Developments in Theory and Experiments*; Schuster, P.; Zundel, G., Sandorfy, C., Eds.; North-Holland: Amsterdam, 1976; Vol. II, p 695.
(18) Hayd, A.; Weidemann, E. G.; Zundel, G. *J. Chem. Phys.* **1979**, *70*, 86.
(19) Weidemann, E. G.; Hayd, A. *J. Chem. Phys.* **1977**, *67*, 3713.
(20) Langner, R.; Zundel, G. *J. Chem. Soc., Faraday Trans.* **1995**, *91* (21), 3831.
(21) Hadži, D. *Pure Appl. Chem.* **1965**, *11*, 435.
(22) Hadži, D.; Kobilarov, N. *J. Chem. Soc.* **1966**, 439.
(23) Zundel, G. *Hydration and Intermolecular Interaction − Infrared Investigation with Polyelectrolyte Membranes*; Academic Press: New York, 1969; p 124.
(24) Krämer, R.; Zundel, G. *J. Chem. Soc., Faraday Trans.* **1990**, *86* (2), 301.
(25) Reinhardt, H.; Bianchi, D.; Mölle, D. *Chem. Ber.* **1957**, *90*, 1656.
(26) Kosolapoff, G. M.; Watson, R. M. *J. Am. Chem. Soc.* **1951**, *73*, 5466.
(27) Hemmer, R.; Lürken, W. *Methoden der Organischen Chemie* (Houben Weyl); Klamann, D., Ed.; Georg Thieme Verlag: Stuttgart, 1992; Band E16d, p 665.